Comparison of the Extensional and Shear Viscosity Characteristics of Aqueous Hydroxyethylcellulose Solutions

J. Meadows,* P. A. Williams, and J. C. Kennedy

North East Wales Institute, Faculty of Science, Health and Medical Studies, Centre for Water Soluble Polymers, Connah's Quay, Clwyd CH5 4BR, U.K.

Received August 4, 1994; Revised Manuscript Received January 23, 1995[⊗]

ABSTRACT: The extensional viscosity characteristics of aqueous solutions of varying concentrations of three samples of hydroxyethylcellulose (HEC) of differing molecular masses have been determined using a commercially available opposed jet extensional rheometer. The results have been compared to the shear flow characteristics of the solutions and the Trouton ratio, T_R, of the various systems calculated. For all polymer solutions studied, T_R was found to approach the predicted Newtonian value of 3 at low extensional strain rates. This observation was taken as a strong indication that the opposed jet rheometer was producing reliable extensional viscosity data. At higher strain rates, T_R generally increased with increasing strain rate and, for any given sample, with increasing polymer concentration thereafter. All HEC solutions studied were found to exhibit strain-thinning behavior in extensional flow and shear-thinning behavior in shear flow, with the most pronounced effects being observed with the highest molecular mass sample ($M_v \sim 4.5 \times 10^5$ g/mol). The relative degrees of strain and shear thinning exhibited by the various HEC solutions have been quantified using the power law analysis. For the two samples of lowest molecular mass ($M_v \sim 6.5 \times 10^4$ and $\sim 1.9 \times 10^5$ g/mol) the value of a power law index, n, in both extensional and shear flow, was close to unity. For all solutions of the sample of highest molecular mass, the value of n in extensional flow was significantly higher than that observed in shear flow. Regions of apparent strain thickening were observed for a few of the lowest viscosity solutions, but these observations were attributed to the onset of significant inertial effects rather than any coil–stretch transition phenomena.

Introduction

Water soluble polymers are widely used to control the rheological properties of an extensive range of aqueous based formulations, and there is a relatively sound understanding of the influence of various polymer characteristics (e.g. concentration, molecular weight, charge density, molecular conformation, etc.) on the shear flow and viscoelastic properties of such systems. In marked contrast, the extensional flow behavior, in particular of aqueous-based systems, has been scarcely studied and, consequently, is still poorly understood despite the fact that it can be envisaged as having important implications in terms of a number of processing and applicational characteristics. For example, processes such as pumping, pouring, and extrusion can all be expected to involve a significant extensional flow.[1]

Until recently, extensional rheology studies have been hindered by a scarcity of experimental techniques by which extensional flow behavior may be controlled and quantified. However, advances in instrumentation have been made in this area and a number of suitable procedures have now been developed.[1–3] Such improved instrumentation has enabled significant progress to be made in understanding the extensional behavior of polymer melts,[4] but the much lower viscosities associated with polymer solutions necessitate the use of nonequilibrium methods[5] which has presented greater difficulties to their characterization. Very recently, however, Tirtaatmadja and Sridhar[6] have developed a filament-stretching device which enables the steady state extensional viscosity of polymer solutions to be determined, provided that the sample is able to sustain a continuous filament for periods of time of up to several seconds. The problems surrounding extensional viscosity measurements on relatively low viscosity fluids were readily reflected by the differing results[7,8] recently obtained by the various laboratories investigating the extensional flow properties of the "international round robin" rheological fluids M1 and A1, which were non-aqueous solutions of polyisobutylene. Ferguson and Hudson[5] have since demonstrated that such discrepancies between the results obtained from the various instrumental approaches may, to a large extent, be reconciled by consideration of the time scales of the measurements and the strain history of the sample.

While there may still be uncertainty regarding the quantitative comparison of data obtained by the various instrumental techniques, there is sufficient agreement in evidence to illustrate that the extensional rheological properties of polymer solutions can be dramatically different from their shear flow characteristics.[7–10] From these and other considerations, it is evident that a detailed understanding and modeling of the factors influencing the extensional rheological characteristics of polymer solutions must be achieved in order to control the total rheological behavior of a polymer-thickened system.

In this paper, we report a comparison of the extensional and shear flow behavior of aqueous solutions of varying concentrations of three commercial samples of hydroxyethylcellulose of differing molecular masses.

Experimental Section

Materials. Commercial samples of hydroxyethylcelluloses of differing molecular masses were kindly supplied by Aqualon (U.K.) Ltd from their Natrosol 250 series of polymers. All polymers had a quoted molar substitution of hydroxyethyl groups of 2.5. The adopted reference coding, moisture content, intrinsic viscosities, and calculated viscosity average molecular masses of the various samples are given in Table 1.

Instrumentation. The Rheometrics (RFX) fluids analyzer, which is schematically represented in Figure 1, falls into the category of stagnation point devices and utilizes the principle of opposing jets to create an area of intense extensional flow. By means of computer-controlled precision syringes, the fluid

[⊗] Abstract published in *Advance ACS Abstracts,* March 1, 1995.

0024-9297/95/2228-2683$09.00/0

Table 1. Adopted Nomenclature and Characteristics of Hydroxyethylcellulose Samples

adopted code	moisture[a] content (% w/w)	intrinsic[b] viscosity (dL g^{-1})	molecular[c] mass ($\times 10^3$) (g/mol)
HEC-low	5.1	1.67	64
HEC-med	9.0	4.28	190
HEC-high	7.3	9.12	450

[a] Determined gravimetrically. [b] Determined in water at 25 °C. [c] Viscosity average molecular mass calculated from $[\eta]$ using 1.1×10^{-4} and 0.87 as the respective values of K and a in the Mark–Houwink equation.

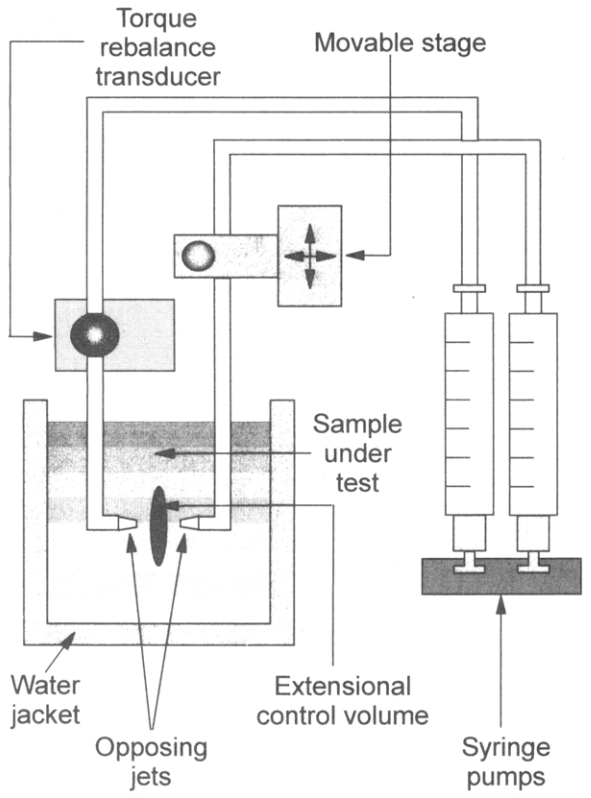

Figure 1. Schematic diagram of the Rheometrics RFX fluids analyzer.

under analysis is drawn into, or expelled through, diametrically opposing jets positioned in a glass beaker containing ~200 cm^3 of the sample fluid. The resulting stresses due to such fluid flow are measured by a torque rebalance transducer (TRT) attached to one of the jet supports, which also acts to maintain the desired separation between the jets. The temperature of the sample fluid is controlled to within ±0.1 °C by circulation of an ethylene glycol/water mixture through the external heating jacket of the beaker.

The determination of extensional viscosity–strain rate profiles is achieved by programming a sequence of desired strain rates into the computer. The instrument generates the desired strain rate through the controlled movement of the syringes and continues to do so until an apparently constant reading is obtained on the TRT. At this point the instrument records the final constant TRT reading, waits at rest for a preprogrammed period, and then proceeds sequentially to the next strain rate. The extensional viscosities of the sample under analysis are calculated from knowledge of the force, jet separation and diameter, and volumetric flow rate as defined below.[11]

Extensional stress:

$$\sigma_e = F_j/A \tag{1}$$

where F_j is the measured force at the jet and A is the cross sectional area of the jet.

Extensional strain rate:

$$\dot{\epsilon} = 8Q/\pi G(D_j)^2 \tag{2}$$

where Q is the volumetric flow rate, G is the gap between the jets, and D_j is the diameter of the jets.

Extensional viscosity:

$$\eta_e = \sigma_e/\dot{\epsilon} \tag{3}$$

By variation of the above parameters, the RFX fluids analyzer is able to determine the rheological characteristics of a sample over four decades of extensional strain rates (~10^{-1}–10^3 s^{-1}). The sensitivity of the torque rebalance transducer enables extensional viscosities of between approximately 10^{-2} and 10^3 Pa s to be measured.

In contrast to the alternative filament-stretching types of extensional rheometers,[2,6] the opposing jet apparatus enables extensional viscosity measurements to be made on fluids, which are not able to sustain a continuous filament. The "nonequilibrium" aspect of the opposed jet technique arises from consideration of the residence times of the polymer molecules within the extensional flow regime. In conventional shear measurements the flow lines of the material are usually "constrained" within the control volume throughout the entire measurement. In contrast, with the opposed jet geometry there will only be a finite length of time between a polymer molecule entering the extensional field and leaving the measurement volume when it is drawn through the jet orifice. Moreover, the actual length of such "residence" time will depend upon the position at which the molecule enters the control volume and will, therefore, vary across the sample. Consequently, there is a degree of uncertainty as to whether the sample has achieved its "true" equilibrium state prior to its measurement. These considerations mean that the extensional viscosities determined by such measurements may more correctly be regarded as the average apparent values.

The established means by which a comparison of the shear and extensional viscosity characteristics of a fluid is normally quantified is through calculation of the Trouton ratio, T_R, which may be defined as

$$T_R = \eta_e(\dot{\epsilon})/\eta(\dot{\gamma}) \tag{4}$$

where η_e is the extensional viscosity of the system at a strain rate $\dot{\epsilon}$ and η is the normal viscosity of the system at the comparable shear rate $\dot{\gamma}$.

For Newtonian fluids, T_R has been theoretically predicted to have a value of 3 which, by definition, is constant over all strain rates. For non-Newtonian systems, calculation of T_R depends on the choice of an appropriate convention by which the strain rates in extensional flow may be related to those in shear flow. Jones et al.[12] have proposed that the appropriate shear rate for use in calculation of T_R should be given by

$$\gamma = \sqrt{3}\dot{\epsilon} \tag{5}$$

and that any deviation away from a Trouton ratio of 3 may be taken as clear evidence of viscoelasticity within the system.

Methods

Preparation of Solutions. All solutions were prepared by adding the appropriate amount of polymer (as received) to a known amount of distilled water followed by overnight tumble mixing to ensure complete dissolution. After mixing, the polymer solutions were stored at 4 °C until analysis which, in all instances, was not more than 48 h after preparation.

In the following text, all polymer concentrations are quoted in % w/w values, based on the weight of dry polymer per weight of solvent (water).

Extensional Measurements. The extensional viscosity–strain rate profiles of the various aqueous polymer solutions were determined at 25 °C using a Rheo-

metrics RFX fluids analyzer. A number of different sets of opposing jets (diameters 1, 2, and 4 mm) were used during the study. In all instances, the maintained distance of separation between the jets was equal to their diameter.

Shear Flow Measurements. The viscosity–shear rate profiles of the various aqueous polymer solutions were determined at 25 °C using a Carrimed CS100 controlled stress rheometer fitted with either a double concentric cylinder or cone and plate measurement geometry.

Results

Double logarithmic scale plots of the extensional viscosity–strain rate and shear viscosity–shear rate profiles of the Newtonian fluid, glycerol at 25 °C, are given in Figure 2, together with the calculated Trouton ratio (T_R). It can be seen that T_R was found to have a value of approximately 3.6 over the entire range of strain rates studied. Similar values for T_R of approximately 4 were also found for ethylene glycol and a standard silicone oil. The slightly, but consistently, higher than predicted value of T_R for Newtonian fluids obtained using the RFX instrument can probably be attributed to the fact that the measured torque is not solely due to the generated extensional flow but also contains additional components. In particular, Schunk et al.[13] have shown there to be a significant momentum transport from outside the region between the two jets. There may also be a certain amount of shear and wall effects occurring near the surface of the jets which also contribute to the measured torque.

Double logarithmic scale plots of the extensional viscosity–strain rate and shear viscosity–shear rate profiles of aqueous solutions of varying concentrations of HEC-high, HEC-med, and HEC-low are given in Figures 3–5, respectively. In all instances, the extensional viscosity of a solution was markedly greater than its shear viscosity over the entire range of deformation rates studied. All solutions were found to exhibit strain-thinning characteristics in extensional flow and shear-thinning characteristics in shear flow, with the most pronounced effects being observed with the highest molecular weight sample. The relative degrees of strain and shear thinning exhibited by the various HEC solutions were quantified by application of the simple power law relationship, which may be expressed as

$$\eta = K_2\dot{\gamma}^{n-1} \tag{6}$$

where η is the viscosity, $\dot{\gamma}$ is the shear rate (or $\dot{\epsilon}$; the extensional strain rate), K_2 is the so-called consistency index, and n is the power law index.

The values of the power law index, n, of the strain- and shear-thinning sections of the various rheological curves illustrated in Figures 3–5 are given in Table 2. For HEC-med and HED-low, both in extension and shear, n was close to unity (>0.9) in all instances and appeared to decrease slightly with increasing polymer concentration. This latter observation was considerably more apparent for the solutions of HEC-high, in particular when considering the shear flow data. For all solutions of HEC-high studied, the value of n in extensional flow was significantly higher than that observed in shear flow, indicating that the solutions of HEC-high were relatively less strain thinning in extensional flow than they were shear thinning in shear flow.

Table 2. Extensional and Shear Viscosity Power Law Exponent, *n*, for Various Aqueous Hydroxyethylcellulose Solutions

polymer	concn (% w/w)	*n* extension	*n* shear	strain/shear rate range (s^{-1})
HEC-high	1.39	0.82	0.48	10^1–10^3
	0.93	0.97	0.57	"
	0.46	0.96	0.79	"
HEC-med	1.82	0.92	0.91	10^0–10^3
	1.37	0.93	0.92	"
	0.91	0.93	0.96	"
	0.46	0.97	0.92	"
HEC-low	3.80	0.92	0.97	10^0–10^3
	2.85	0.94	0.95	"
	1.90	0.97	0.96	"

Table 3. Measurement and Sample Characteristics of Various Aqueous Hydroxyethylcellulose Solutions at the Onset of the Region of Apparent Strain Thickening

polymer	concn (% w/w)	diameter of jet (mm)	$\dot{\epsilon}_{cs}$[a] (s^{-1})	η_e(cs)[b] (Pa s)	R_e[c]
HEC-low	1.90	1	~1000	0.055	9.1
	2.85	1	~1500	0.10	7.5
HEC-med	0.46	1	~400	0.025	8.0
	0.46	2	~100	0.025	8.0
HEC-high	0.46	2	not observed	0.18–0.22	

[a] $\dot{\epsilon}_{cs}$ = extensional strain rate at the onset of the region of apparent strain thickening. [b] η_e(cs) = extensional viscosity of sample at $\dot{\epsilon}_{cs}$. [c] R_e = characteristic Reynolds number for extensional flow of sample at $\dot{\epsilon}_{cs}$.

During the generation of the extensional viscosity–strain rate profiles for the various HEC solutions given in Figures 3–5, there were a number of instances when regions of apparent strain-thickening behavior were observed in the lower viscosity systems (η_e < 0.1 Pa s). These instances are illustrated in the curves given in Figure 6. The measurement and sample characteristics of these systems at the critical strain rate, $\dot{\epsilon}_{cs}$, at which the region of apparent strain thickening commenced are given in Table 3. It can be seen that the characteristic Reynolds number, R_e, of each system at $\dot{\epsilon}_{cs}$ exhibited a high degree of similarity.

In this analysis, R_e was calculated by substitution of the strain rate relationship for the RFX instrument given in eq 2 into the equation given by Hasegawa and Fukutomi[14] to calculate R_e for orifice flow, thereby yielding

$$R_e = \varrho\dot{\epsilon}GD_j/2\eta_e \tag{7}$$

where ϱ and η_e are the density and extensional viscosity of the fluid respectively, $\dot{\epsilon}$ is the extensional strain rate, G is the distance of separation between the jets, and D_j is the diameter of the jets.

The calculated Trouton ratios, T_R, of the various aqueous solutions of HEC are given as a function of strain rate in Figure 7. For all polymers, T_R tended toward the predicted Newtonian value of 3 at low strain rates but generally increased with increasing strain rate and, for any given sample, with increasing polymer concentration thereafter. For solutions of HEC-med and HEC-low, the values of T_R showed a lesser dependence on strain rate and were generally much smaller than those of HEC-high.

Double logarithmic scale plots of specific viscosity against the dimensionless concentration parameter $C[\eta]$ (where $[\eta]$ is the intrinsic viscosity) are given in Figure 8 for the various HEC samples for both extensional and shear flow data. It can be seen that, with the possible exception of HEC low at relatively high concentrations,

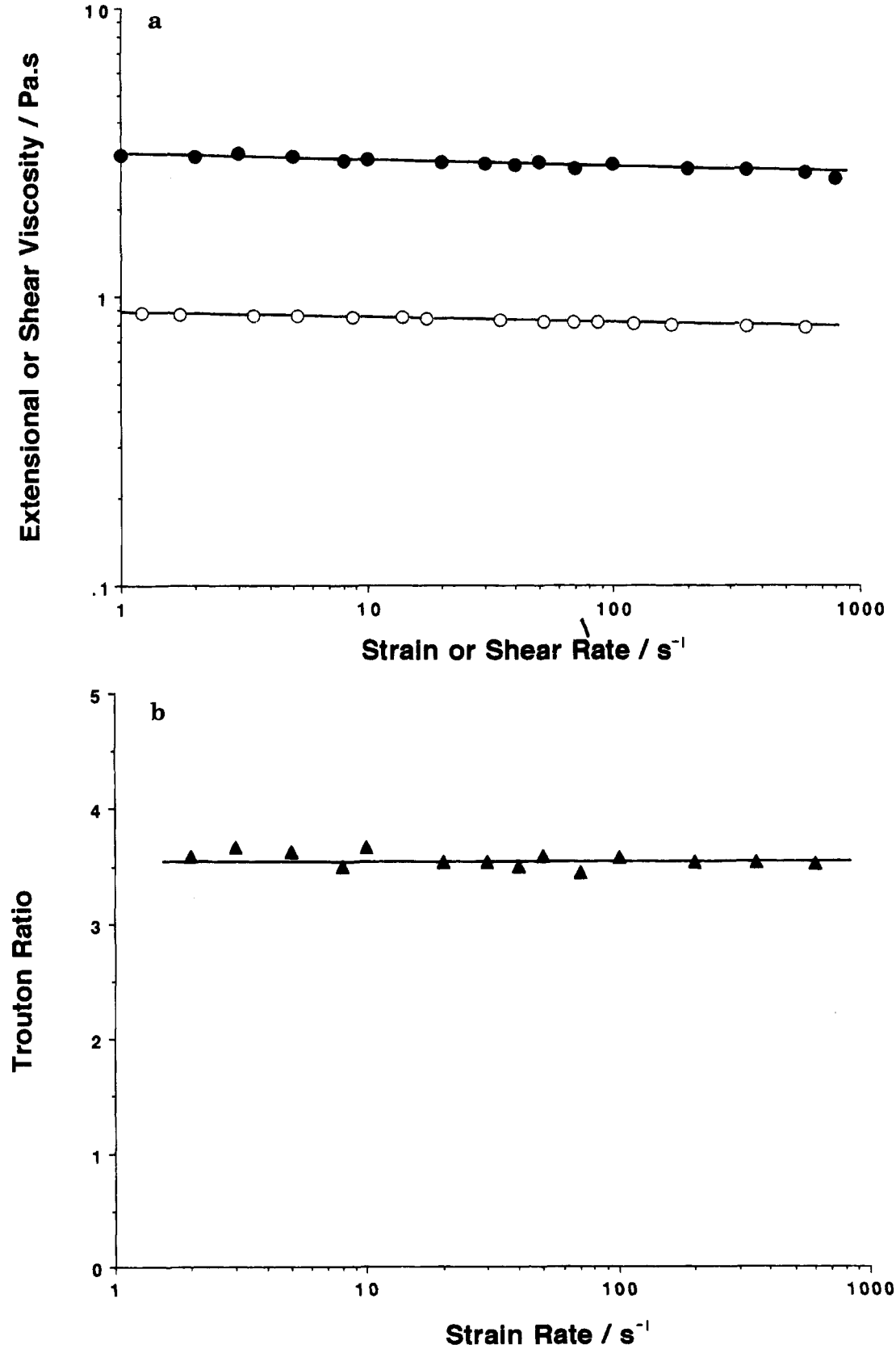

Figure 2. (a) (●) Extensional viscosity–strain rate and (○) shear viscosity–shear rate and (b) (▲) Trouton ratio–strain rate profiles of Glycerol at 25 °C.

the plots for the various HEC samples in both flow regimes are largely superimposible and fall on a single "master" curve. The relatively small number of extensional flow data points incorporated in Figure 8 is a reflection of the narrower range of sample capability of the RFX instrument compared to the controlled stress rheometer used to generate shear flow data in this study. It should be noted that while the shear flow data points shown represent experimentally determined zero shear viscosity values, the extensional flow data points correspond to viscosity values determined at the extensional strain rate of 2 s^{-1}. Furthermore, in the calcula-

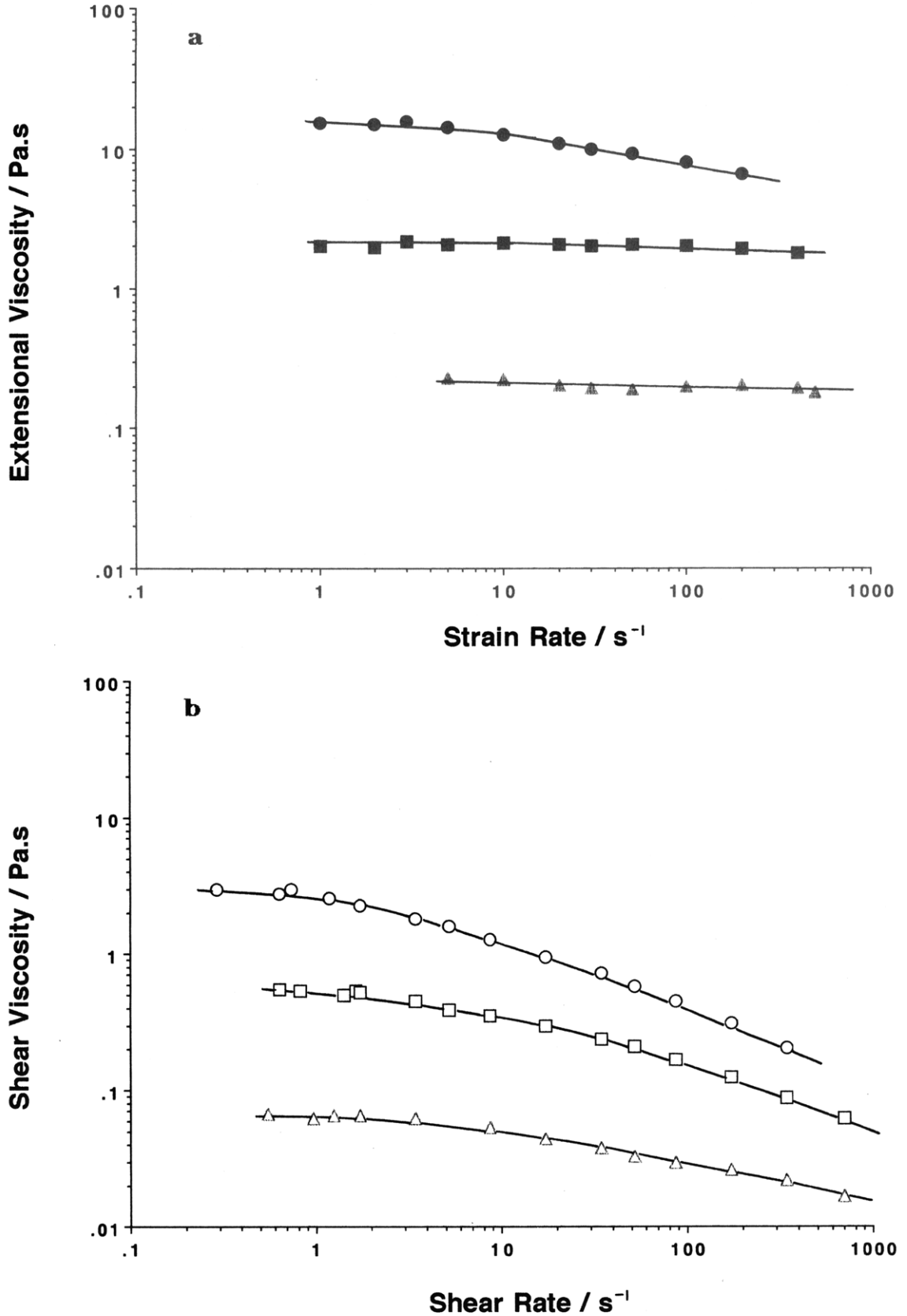

Figure 3. (a) Extensional viscosity–strain rate (filled symbols) and (b) shear viscosity–shear rate (open symbols) profiles of aqueous solutions of varying concentrations of HEC-high: (●, ○) 1.39%; (■, □) 0.93%; (▲, △) 0.46%.

tion of the specific extensional viscosities, the appropriate extensional viscosity of water was taken to be 3 times its shear viscosity (Newtonian fluid).

Discussion

Hydroxyethylcellulose is a conventional soluble polymeric thickener which builds viscosity in a solvent phase through simple molecular entanglements. The reduction in bulk viscosity of the HEC solutions with increasing shear rate (Figures 3–5) is typical for the majority of polymer solutions and can be attributed to the progressive mechanical disruption of intermolecular

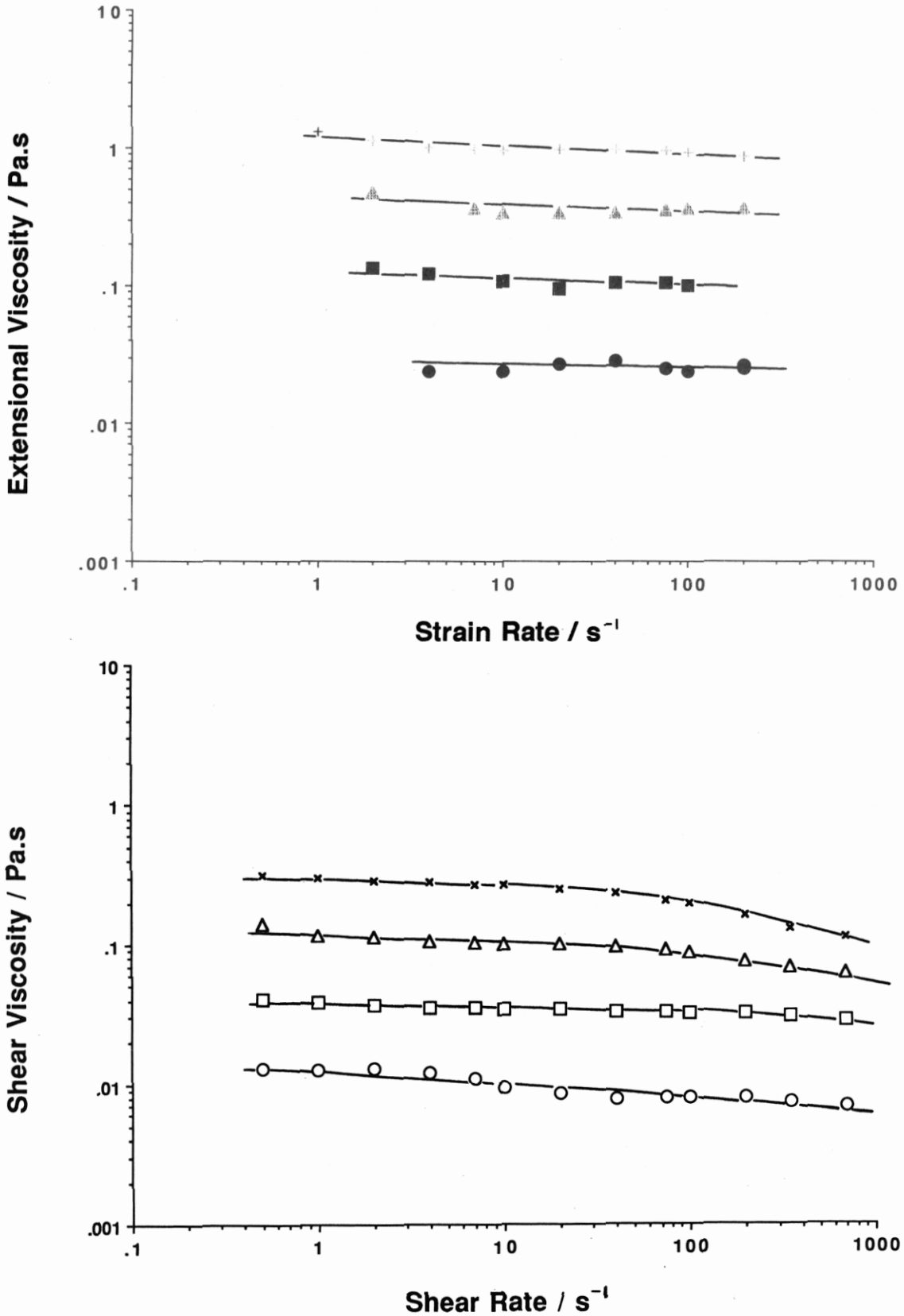

Figure 4. (a) Extensional viscosity–strain rate (filled symbols) and (b) shear viscosity–shear rate (open symbols) profiles of aqueous solutions of varying concentrations of HEC-med: (+, ×) 1.82%; (▲, △) 1.37%; (■, □) 0.91%; (●, ○) 0.46%.

entanglements and deformation of polymer coils. In contrast, under an extensional flow field, flexible chain molecules are expected to exhibit strain-hardening characteristics over at least part of the deformation regime. The observation that the HEC solutions investigated in this study actually exhibited slight strain-thinning behavior may be attributed to the "stiffer" conformation of the cellulosic polymers, thereby restricting the extent of any "coil–stretch" associated strain hardening. However it should also be noted that the HEC solutions investigated in this study were all above their critical coil overlap concentration and thus it is also possible that the cumulative strain-hardening effects of individual polymer molecules were offset by

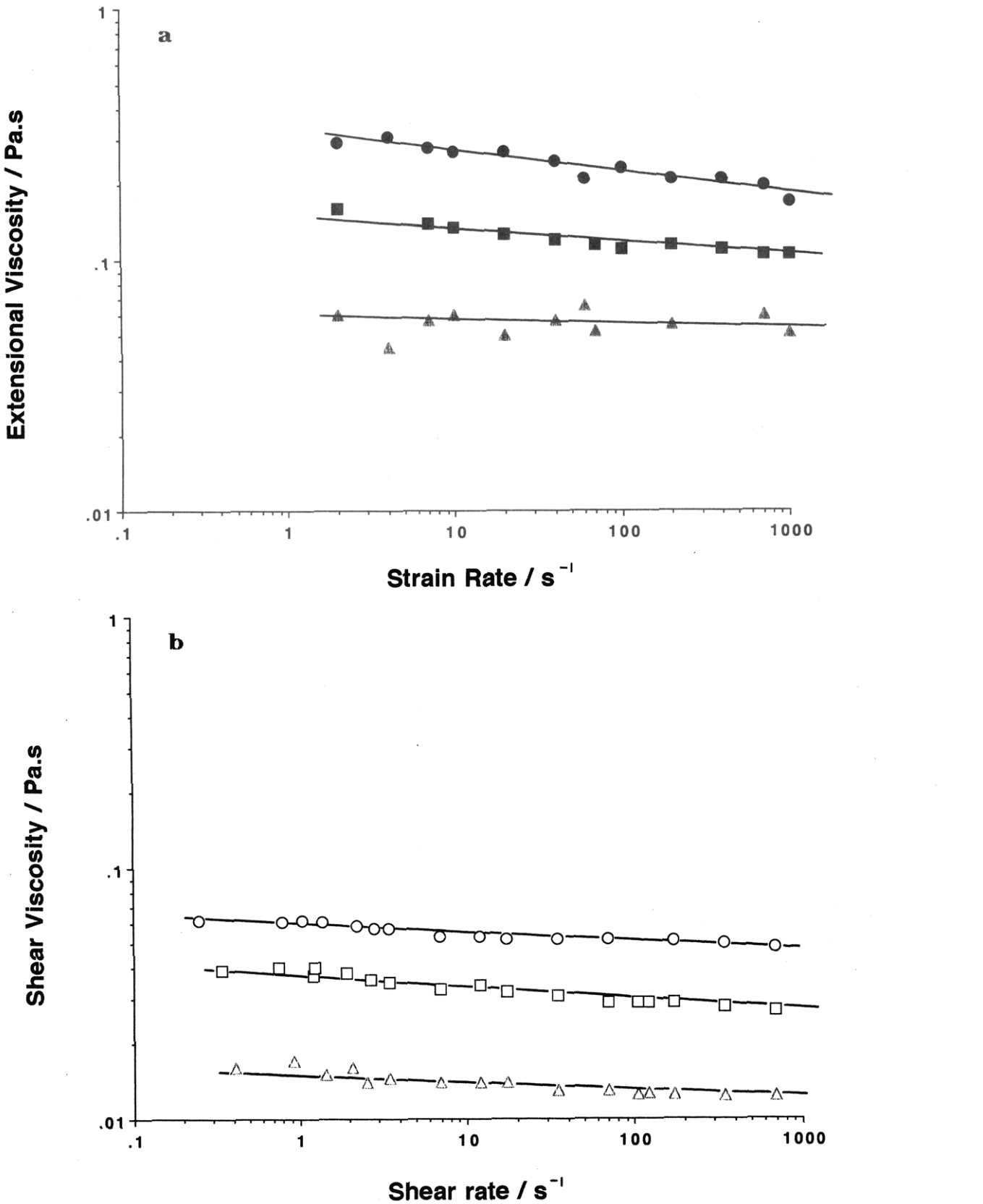

Figure 5. (a) Extensional viscosity–strain rate (filled symbols) and (b) shear viscosity–shear rate (open symbols) profiles of aqueous solutions of varying concentrations of HEC-low: (●, ○) 3.80%; (■, □) 2.85%; (▲, △) 1.90%.

the strain-thinning effects of the mechanical disruption of intermolecular entanglements.[15]

For shear flow, there have been a variety of relationships developed to describe the overall viscosity–shear rate profile of a polymer solution. However, analogous relationships have not yet been developed for extensional flow and, thus, comparison of shear and extensional flow data can presently only be achieved through application of suitable shear-based models to both flow regimes. While the Cross model[16] is one of the most commonly used equations to describe shear flow data, its application necessitates the knowledge, estimation,

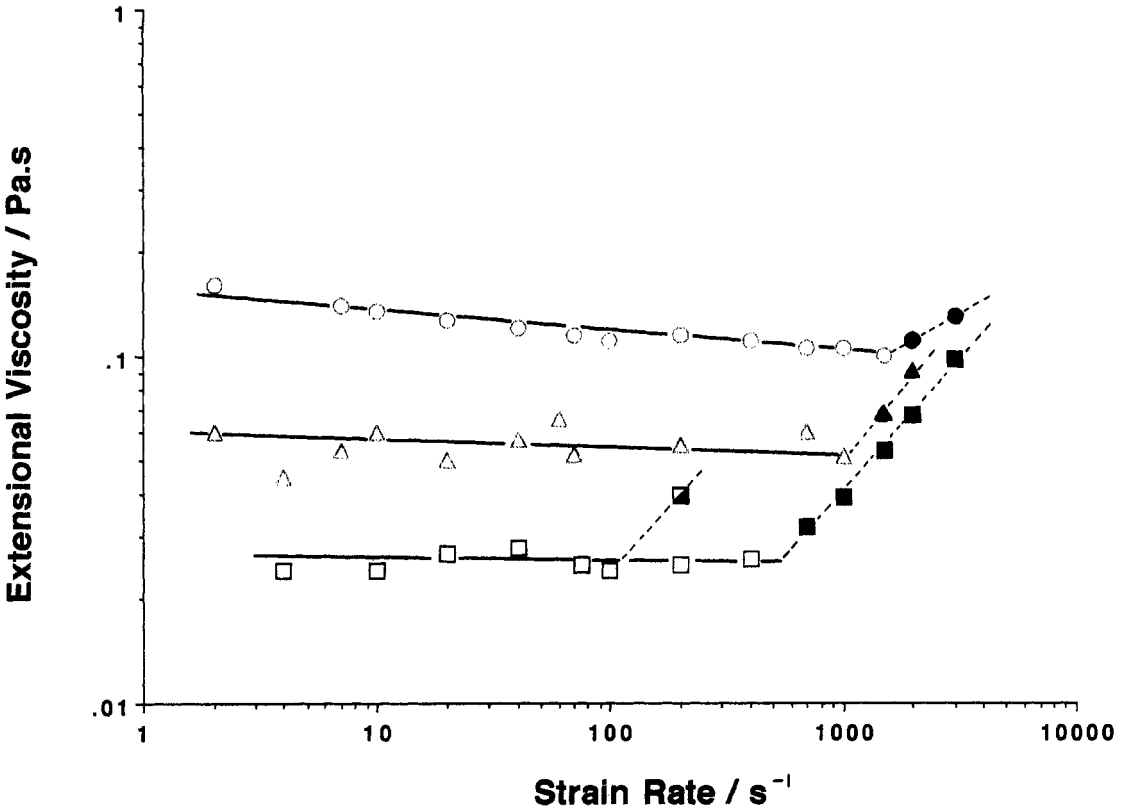

Figure 6. Examples of the occurrence of regions of apparent strain thickening (filled symbols) in the extensional viscosity strain rate profiles of various aqueous solutions of HEC: (●) 2.85% HEC-low (1 mm jet); (▲) 1.90% HEC-low (1 mm jet); (◪) 0.46% HEC-med (2 mm jet); (■) 0.46% HEC-med (1 mm jet).

or assumption of the values for both the low- (η_0) and high-shear (η_∞) Newtonian plateau viscosities. From the rheological data for the HEC solutions given in Figures 3–5, it is clear that while values of η_0 may be generated for the HEC solutions in shear flow, the lack of experimental or relevent literature data means that it is very difficult to anticipate how the extensional flow curves of the HEC solutions would continue at lower strain rates, thus preventing the estimation of η_0 in extensional flow. In addition, the values for η_∞ for the various HEC solutions were not experimentally accessible or confidently predictable in either flow regime.

In contrast to the more extensive Cross model, power law relationships describe only the mid-shear section of the overall flow curve and do not require values for either of the apparent Newtonian plateau viscosities. The evidently lower values of the power law index, n, for the solutions of HEC-high compared to solutions of either of its two lower molecular mass counterparts can be attributed to the larger number of intermolecular entanglements initially present in the former system. Though it is recognized that shear and extensional flow represent quite different modes of deformation of the polymer solution, the general observation that, for a given system, the values of the power law index in extensional flow were somewhat higher than in shear flow may be indicative of the higher number of intermolecular entanglements and "contacts" that could be expected to occur between directionally aligned extended chains in extensional flow compared to mechanically deformed random coils in shear flow.

The occurrence, above an apparently critical extensional strain rate, of strain-thickening extensional viscosity profiles, such as those illustrated in Figure 6, has been predicted and observed for dilute solutions of random coil polymers.[17–19] Such a phenomenon is proposed to arise from the strain-induced "stretching" of the initially compact polymer coil to a more extended conformation, thereby resulting in an increased drag. Rabin[17] has proposed that the critical strain rate, $\dot{\epsilon}_{cs}$ at which the "coil–stretch" transition occurs should scale with the molecular weight of the polymer according to the relationship

$$\dot{\epsilon}_{cs} \propto M^{-1-\upsilon} \tag{8}$$

where is υ the Flory exponent and has the values of 0.6 and 0.5 in good and Θ solvents, respectively.

When the extensional viscosity data given in Figure 6 and Table 3 are considered, there are a number of evident problems concerning the application of Rabin's proposed scaling relationship. Firstly, there appears to be a concentration dependence in the values for the apparent $\dot{\epsilon}_{cs}$ of HEC-low. Secondly, there is a marked dependence of $\dot{\epsilon}_{cs}$ upon the measurement geometry for the 0.46% solution of HEC-med. Finally, on the basis of the data given in Figure 6 and Table 3, one would anticipate the occurrence of $\dot{\epsilon}_{cs}$ at even lower strain rates for the 0.46% solution of HEC-high. However, no such strain-thickening regime is evident in the extensional viscosity profile for this system given in Figure 3. These observations suggest that, apart from any "coil–stretch" transition phenomena, other factors, perhaps some form of flow instability, may be responsible for the regions of apparent strain-thickening behavior illustrated in Figure 6.

The characteristic Reynolds number, R_e, expresses the ratio of the inertial and viscous forces of a fluid under flow. If this ratio is too large, then inertial effects can influence measurements and must be considered in any data interpretation. From eq 7, it can be seen that, for the flow of a strain-thinning fluid through any particu-

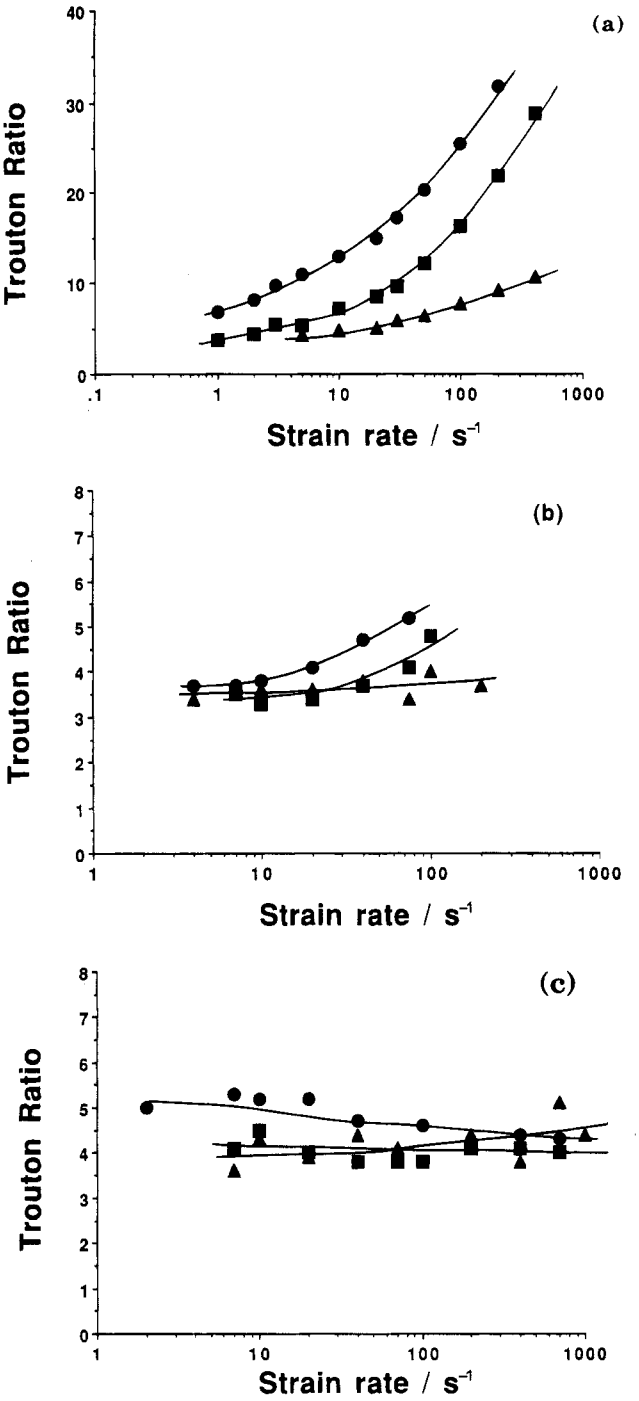

Figure 7. Trouton ratio–strain rate profile of aqueous solutions of varying concentrations of various samples of HEC: (a) HEC-high (●) 1.39%, (■) 0.93%, and (▲) 0.46%; (b) HEC-med (●) 1.82%, (■) 1.37%, and (▲) 0.46%; (c) HEC-low (●) 3.8%, (■) 2.85%, and (▲) 1.90%.

lar jet, R_e will increase with increasing extensional strain rate. We believe that the strong similarity in evidence in Table 3 between the values of R_e for the various solutions at $\dot{\epsilon}_{cs}$, together with the inconsistencies in data interpretation described above, strongly suggests that the apparent strain-thickening phenomenon illustrated in Figure 6 is artifactual and actually corresponds to the onset of turbulent flow. From the data given for HEC in Table 3 and other, as yet unpublished, data which we have generated concerning the extensional viscosity characteristics of a number of other water soluble polymers such as sodium carboxymethylcellulose, hydroxybutylguar, and hydrophobically modified polyelectrolytes, it appears that for the RFX instrument, inertial effects cease to be negligible once a critical value of approximately 5 for R_e for the fluid under analysis has been exceeded.

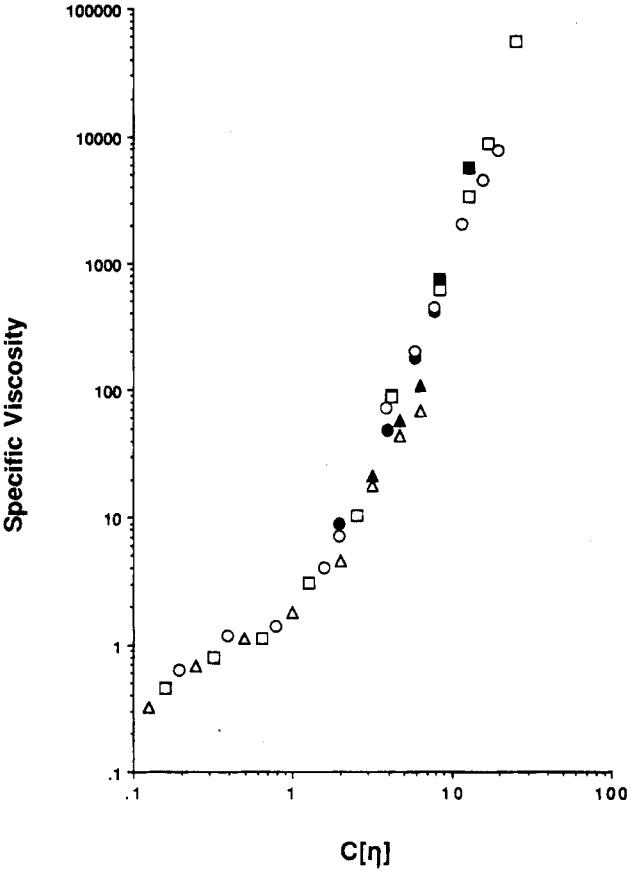

Figure 8. Plots of the specific viscosity against the dimensionless concentration parameter $C[\eta]$ for aqueous solutions of various HEC samples in shear flow (open symbols) and extensional flow (closed symbols): (■, □) HEC-high; (●, ○) HEC-med; (▲, △) HEC-low.

The general increase in Trouton ratio of the various HEC solutions, in particular those of HEC-high, illustrated in Figure 7 is a consequence of the relatively lower strain rate dependence of the extensional viscosity of the HEC solutions compared to the shear rate dependence of their shear viscosities (as quantified in Table 2 by the differing power law indices in extension and shear). The data given in Figure 7 show that at high strain rates the extensional viscosity of the higher concentrations of HEC-high solutions studied were more than 30 times the value of their comparable shear viscosities. This observation emphasizes the potential importance of extensional viscosity characteristics in determining the overall rheological behavior of a polymer solution. The reduced strain rate dependence and generally lower values of T_R for the solutions of HEC-med and HEC-low are indicative of a more Newtonian-like behavior of solutions of these lower molecular weight polymers, as also indicated by the relatively high and similar values of their power law indices in extension and shear (Table 2).

In addition to being a further indication that the RFX instrument is generating reliable extensional viscosity measurements, the fact that the extensional data points for the HEC solutions fall on the shear flow "master" curve given in Figure 8 suggests that the extensional viscosity values at the strain rate of 2 s^{-1} must closely resemble the values of any apparent Newtonian plateau

evident at lower strain rates. This inference is not too surprising given the relatively low degree of extensional thinning behavior exhibited by the HEC solutions (Table 2).

When considering the interpretation of rheological "master" curves analogous to that given in Figure 8, the majority of workers[20,21] have analyzed their data in terms of the two straight line approximation, with the intersect $C[\eta]_{cr}$ being widely viewed as representing the onset of the semidilute regime of the polymer solution. In contrast, however, Launay and co-workers[21,22] have proposed that the evident nonlinearity of such plots in the vicinity of $C[\eta]_{cr}$ means that the data should be better treated by the combination of three adjoining straight lines and two critical polymer concentrations, $C[\eta]^*$ and $C[\eta]^{**}$, corresponding to the existence of, and the transitions between, the so-called dilute, semidilute, and concentrated regimes. The initial critical concentration $C[\eta]^*$ is assigned to the onset of significant coil overlap. In the ensuing semidilute regime, a progressive contraction of the coils is proposed to occur due to the presence of the increasing number of other polymer molecules. Such contraction continues to occur until the coils have attained essentially their unperturbed dimensions, at which point ($C[\eta]^{**}$) the onset of a third "concentrated" regime may be defined in which the dimensions of the polymer coils become independent of concentration. For any given system, the value of $C[\eta]_{cr}$ obtained from a two-line analysis will always fall between the values of $C[\eta]^*$ and $C[\eta]^{**}$ obtained from a three-line analysis.

Although there is a degree of variation in the values of $C[\eta]_{cr}$ reported by different authors using the two-line analysis, it is usually found to be in the range of 2−4 and the respective gradients a_1 and a_2 of the plots below and above $C[\eta]_{cr}$ are found to be in the ranges 1−1.5 and 3−5, respectively.[21] The experimental scatter evident in the data given in Figure 8 make it difficult to unambiguously distinguish between the relative merits of either the two- or three-line analysis. However, it is apparent that the rheological data generated for the HEC solutions within this study are in broad agreement with the reported literature for a wide variety of aqueous polysaccharide systems.

Conclusions

The Rheometrics RFX fluids analyzer has been shown to be a reliable means of obtaining semiquantitative comparisons of the extensional viscosities of relatively low viscosity fluids. On a cautionary note, however, above an effective Reynolds number for the measurement flow of approximately 5, it would appear that inertial effects begin to be significant, giving rise to anomalous regions of apparent strain thickening in low-viscosity fluids.

Acknowledgment. The authors would like to express their gratitude to SERC (Process Engineering Committee) for the provision of a Cooperative Research Grant (GR/H79648) in conjunction with Allied Colloids Ltd., U.K., which enabled this work to be undertaken.

References and Notes

(1) Barnes, H. A.; Hutton, J. F.; Walters, K. *An Introduction to Rheology*; Elsevier Science Publications: Amsterdam, 1989; pp 75−96.
(2) James, D. F.; Walters, K. In *Techniques in Rheological Measurement*; Collyer, A. A., Ed.; Elsevier: New York (to be published).
(3) Ferguson, J.; Walters, K.; Wolff, C. *Rheol. Acta* **1990**, *29*, 571.
(4) Meissner, J. *Ann. Rev. Fluid Mech.* **1985**, *17*, 45.
(5) Ferguson, J.; Hudson, N. E. *Eur. Polym. J.* **1993**, *29*, 141.
(6) Tirtaatmadja, V.; Sridah, T. *J. Rheol.* **1993**, *37*, 1081.
(7) Sridhar, T. *J. Non-Newtonian Fluid Mech.* **1990**, *35*, 85.
(8) Hudson, N. E.; Jones, T. E. R. *J. Non-Newtonian Fluid Mech.* **1993**, *46*, 69.
(9) Barnes, H. A. *Polym. Mater. Sci. Eng.* **1989**, *61*, 30.
(10) Vissmann, K.; Bewersdorff, H. W. *J. Non-Newtonian Fluid Mech.* **1990**, *34*, 289.
(11) Fuller, G. G.; Cathey, C. A.; Hubbard, B.; Zebrowski, B. E. *J. Rheol.* **1987**, *31*, 235.
(12) Jones, D. M.; Walters, K.; Williams, P. R. *Rheol. Acta* **1987**, *26*, 20.
(13) Schunk, P. R.; de Santos, J. M.; Scriven, L. E. *J. Rheol.* **1990**, *34*, 387.
(14) Hasegawa, T.; Fukutomi, K. *Proc. Xth International Congress on Rheology*, Sydney; 1988, p 395.
(15) Meadows, J.; Williams, P. A.; Kennedy, J. C. Manuscript in preparation.
(16) Cross, M. M. *J. Colloid Sci.* **1965**, *20*, 417.
(17) Rabin, Y. *J. Non-Newtonian Fluid Mech.* **1988**, *30*, 119.
(18) Larson, R. G. *Rheol. Acta* **1990**, *29*, 371.
(19) Georgelos, P. N.; Torkelson, J. M. *Rheol. Acta* **1988**, *27*, 369.
(20) Morris, E. R.; Cutler, A. N.; Ross-Murphy, S. B.; Rees, D. A.; Price, J. *Carbohydr. Polym.* **1981**, *1*, 5.
(21) Launay, B.; Doublier, J. L.; Cuvelier, G. In *Functional Properties of Food Macromolecules*; Mitchell, J. R., Ledward, D. A., Eds.; Elsevier Applied Science: London, 1986; p 1.
(22) Launay, B.; Cuvelier, G.; Martinez-Reyes, S. In *Gums and Stabilisers for the Food Industry 2*; Phillips, G. O., Wedlock, D. J., Williams, P. A., Eds.; Pergamon Press: Oxford, U.K., 1984; p 79.

MA945094+